Proceedings of the 9ICEG
9th International Congress on Environmental Geotechnics
25-28 June, 2023 | Chania, Greece

https://doi.org/10.53243/ICEG2023-95

Modeling of Semi-mechanistic approach for Geo-synthetic Reinforced Flexible Pavement Design

Prabhakar Vishwakarma[1], and Siva Ram Karumanchi[2]

[1]*Research scholar, IIT Gandhinagar, India, email: prabhakar.18350004@iitgn.ac.in*

[2]*Post doctoral fellow, IIT Gandhinagar, India, email: s.karumanchi@iitgn.ac.in*

ABSTRACT

Reinforced flexible pavement is being constructed to increase pavement service life and make optimal use of geosynthetics. Appropriate selection of geogrid stiffness within the asphalt concrete layer and proper choice of subgrade materials may lead to a workable solution. Rut depth estimation under the various contact pressure with the varying subgrade modulus is the best approach to identifying the suitable geogrids range. A 2D axis-symmetrical numerical model was developed to simulate the typical pavement response under heavy traffic loading. Elasto-plastic behavior of soil material was considered for the base and subgrade layer. Initially, the developed numerical model was validated with the published experimental simulations, and the obtained numerical results are in good agreement with the experimental results. Further, this study presents the estimation of rut depth for the various subgrade modulus, cyclic wheel loading, and geogrid stiffnesses from the numerical simulations. The results show the beneficial effect of the appropriate range of geogrid stiffness in the asphalt concrete layer. Qualitative discussions are made from parametric analyses on the variation of vertical surface deformations of reinforced flexible pavements under repeated wheel loading. The results indicated that the rut depth increased for pavements with a lower subgrade modulus. However, this study observes a significant reduction in pavement's rut depth with varying geogrid stiffness from 100 kN/m to 400 kN/m. Thus, selecting geogrid with a stiffness greater than 400 kN/m is advisable for the better long-term performance of the pavements having lower subgrade modulus.

Keywords: Geogrids, rut depth, pavement, numerical model, subgrade modulus

1 INTRODUCTION

The effectiveness and quality of road surfaces impact people's quality of life, the stability of the social system, and the continuation of economic and commercial operations, yet road pavement surfaces show wear and tear from a continuous operation. Defects in the pavement arise as a result of the combined effects of traffic loading and environmental factors, a process known as pavement surface deterioration (Adlinge & Gupta, 2013). Wheel loads repeatedly experienced by vehicles result in traffic loads, which can lead to pavement elements failing structurally or functionally (Behiry, 2012). Climate-related factors like temperature changes or moisture in the subgrade produce environmental loads that might lead to surface imperfections and structural strain (Kodippily et al., 2020). The road's serviceability, safety, and ride quality are all significantly impacted by pavement deterioration (which necessitates reactive repairs, road closures, and expensive resurfacing). The pavement structure is susceptible to several types of distress throughout its lifetime.

Cracking and rutting are the two basic types of flexible pavement distress mechanisms. Cracking affects asphalt pavement surfaces (Yin, 2010). For this reason, in many countries, cracking performances and rutting are incorporated into pavement road design and maintenance systems. The reinforced pavement performance significantly improved using appropriate geogrids and geotextiles (Collin et al.1996). Perkins & Ismeik (1997) studied the geosynthetics reinforcement of base course on unpaved roads to increase the bearing capacity with a tolerance rut depth of 25 mm. Cancelli et al. (1996) used five different types of geogrids and one geotextile. The stiffness and the manufacturing process of the geogrids have differed, significantly impacting the reinforcement performance. Sprague et al. (2004) studied using geogrid in flexible pavement construction to reinforce the aggregate base course over soft subgrade soils. They recognized the importance of confinement of the base course

by a geogrid from the measurements of small-scale tests. Further, Perkin et al. (2007) proposed a mechanistic-empirical model for geosynthetic base-reinforced flexible pavement. They described the basic components of the model with a focus on the ability to predict permanent deformation compared to the test sections' results. Suku et al. (2012) developed a numerical approach to evaluate geocell use in flexible pavements. Their study includes the influence of geocells on the required pavement thickness by placing it below the granular layers and above the subgrade. Taherkhani & Jalali (2017) evaluated the effectiveness of geosynthetics to reduce the critical strains in the flexible pavement under various dynamic axle load levels and using geogrid stiffness of different values using ABAQUS. The pavement mechanical response was significantly affected when adding the geogrid between the asphalt concrete layers.

Recent geocell modeling applications for pavement construction propose the geocell-soil composite to be the pavement layer with enhanced strength and stiffness characteristics (Maheshwari & Babu, 2017). Although these techniques are quite simple, it is impractical to model geocells as the soil layer when simulating the issue of the single-cell geocell exposed to uniaxial compression. Hegde & Sitharam (2015) utilized the circular-shaped pocket geometry for the numerical assessment of geocell-reinforced pavements. They showed the need to accurately simulate the real form of the geocells and its accuracy in the simulation results. Further, Arias et al. (2020) evaluated the performance of geocell-reinforced pavements concerned with probable heavy loads. Ari & Misir (2021) used PLAXIS 3D to replicate the geocell honeycomb geometry and stiff body behavior. Shell foundations resting on geocell-reinforced sandy beds were added to the verified models. Adding geocell reinforcement reduced the settlement of pyramidal and conical shell foundations by more than 70%. Compared to the unreinforced examples, the stress transferred to the sand beds was reduced and distributed over a larger region. These discussions indicate the improved performance of pavements using geogrid and geocell on-road sections. Here, an attempt has been made to analyze the response of various geogrids using numerical simulation to optimize the reinforcement requirements for the better performance of pavements. The numerical modeling is validated using experimental findings. In addition, the validated numerical model describes the influence of different geogrid properties on the stiffness of various pavement layers. This work primarily emphasizes numerical simulations of pavement geogrids that carefully consider layer stiffness. Semi-mechanistic approaches are applied in the pavement layers to improve their engineering performances, such as reducing pavement layers, improving resilient modulus, and reducing the rutting depth.

2 FINITE ELEMENT ANALYSIS OF FLEXIBLE PAVEMENT WITH GEOGRID

Reinforced flexible pavement is being constructed to increase pavement service life and make optimal use of geosynthetics. Appropriate selection of geogrid stiffness within the asphalt concrete (AC) layer and proper choice of subgrade materials may lead to a workable solution. Rut depth estimation under the various contact pressure with the varying subgrade modulus is the best approach to identifying the suitable range for using geogrids. Using the ABAQUS software, a two-dimensional (2D) finite element tool was used to model a typical pavement section assuming plain strain conditions. The mohr-Columb model was used for the base layer and subgrade materials. The beam element is used for geogrids to simulate the interaction condition with the rough interfaces. In the present study, the axisymmetric model is used to validate the experimental result (Correia et al. 2018) in the presence of geogrids. The repeated wheel loads were simulated in the Finite Element model. The finite element results show the effect of subgrade modulus, contact pressure, and geogrid stiffness on the rut depth. Table-1 represents the different types of geogrid used for the tensile strength (derived from stiffness) ranging from 19 to 900 kN/m. These strength values are obtained from the respective manufacturer's sheets. The layer's property in the model is illustrated in Table-2 (Correia et al. 2014; Al-Jumaili et al. 2016).

Table 1. *Typical range of geogrid tensile strength derived from stiffness*

Geogrid used in Pavement	Tensile Strength (kN/m)
BPM Plastic Biaxial geogrid (@ 2% strain)	40
Tensar BX4200 (@ 5% strain)	20.5
Tensar TriAx Tx 130s (@ 0.5% strain)	200
Tensar TriAx Tx 170s (@ 0.5% strain)	500
Carthage Mills GBX®-12 (@ 5% strain)	19.2
Fiberglass geogrid	150

Table 2. *Material properties in numerical simulation (*Correia et al. 2018*)*

Material	AC layer	Base course	Subgrade
Constitutive mode	Linear elastic	Mohr-coulomb	Mohr-Coulomb
Thickness	110 mm	200 mm	100mm
Young's Modulus	2500 Mpa	100 MPa	10 MPa
Unit weight	25 kN/m3	22	18
Poisson's ratio	0.35	0.3	0.4
Cohesion (kPa)		0.01	46
Friction angle		45	26
Damping		α = 0.55 β =	α = 0.55 β = 0.0001

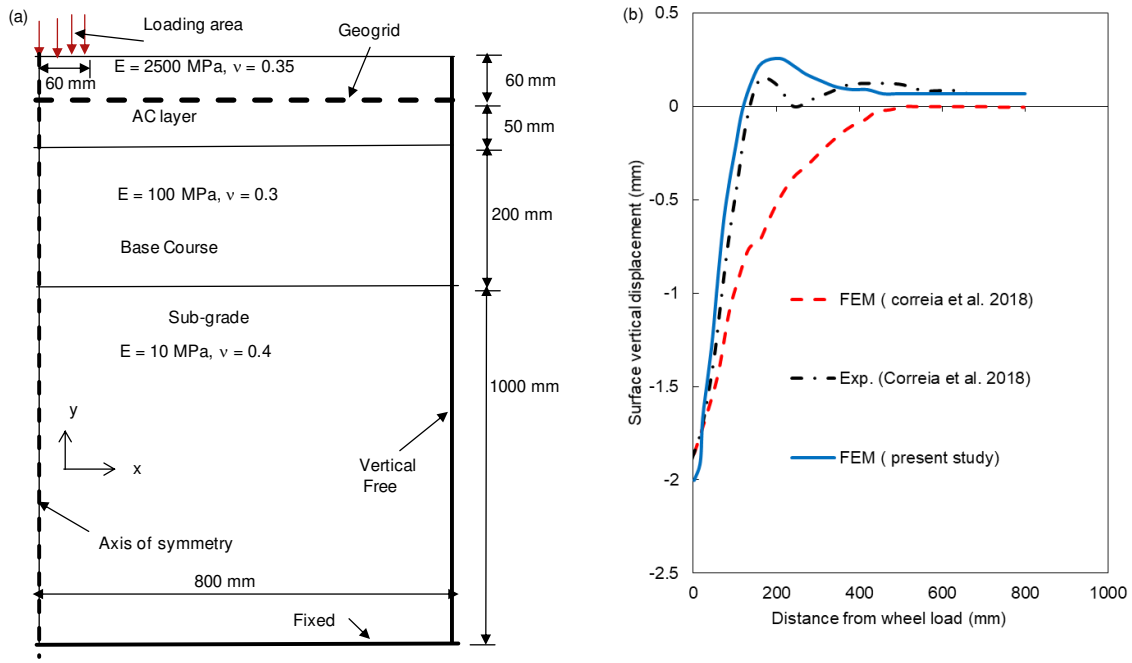

Figure 1. *2D geometry used for Finite Element Model (left), Comparison of Correia et al. 2018 result with FEM (right)*

Figure 1a shows the two-dimensional (2D) geometry for the finite element model. The mesh size of 0.06 m is used with the quad element. As the virtue of symmetricity, only half of the pavement system is simulated. The vertical sides of the mesh are restrained only in the x-direction, whereas the bottom side is assumed to be restrained in both the x and y-directions. The interaction between the geogrid and asphalt layers was simplified by assuming full bonding between AC layers with the rough surface (Ling et al. 2003; Rota et al. 2011). The loading condition was simulated by applying a contact pressure of 700 kPa (Correia et al. 2014 and Al-Jumaili et al. 2016). The result obtained from the numerical predictions were compared with the experimental result (Correia et al. 2014) to validate the numerical model. The developed finite element (FE) model accurately predicted the displacement along the width of the pavement. A circular contact area with a radius of 0.06 mm is considered in the axisymmetric model, and 8000 N (1/5 of 40,000, which IRC recommends: 37-2018) load was applied.

The validation of the model is essential to proceed further in any analysis. Figure. 1b presents the experimental (Correia et al. 2018) and predicted (FEM using ABAQUS) rutting profile (i.e., vertical surface displacement) under the contact pressure of 700 kPa. In the present study, reinforcements are embedded in the pavement model. The depicted results indicated a good agreement with the experimental results of Correia et al. 2018. Further, the difference in numerical results between Correia et al. 2018 and the present numerical study indicates the impact of embed conditions of reinforcement, which is one of the critical parameters that govern the load–displacement behavior of reinforced pavements.

3 Analysis

Figure 2a shows the result of a parametric evaluation illustrating the effect of subgrade modulus in the pavement model under the wheel pressure of 200, 500, and 700 kPa. There is minimal change in rut depth for the subgrade modulus, which ranges from 50 to 100 MPa. So using subgrade material with 5% California bearing ratio (CBR) is optimal for locally available soil (IRC-37 2018), which also represents the weak subgrade condition (Correia et al. 2018). Figure 2b presents the rate of change of rut depth with the wheel contact pressure of 200 to 1000 kPa. There is a significant change in the rut depth for the lower subgrade modulus of 50 and 100 MPa pattern of change is very less for the subgrade modulus.

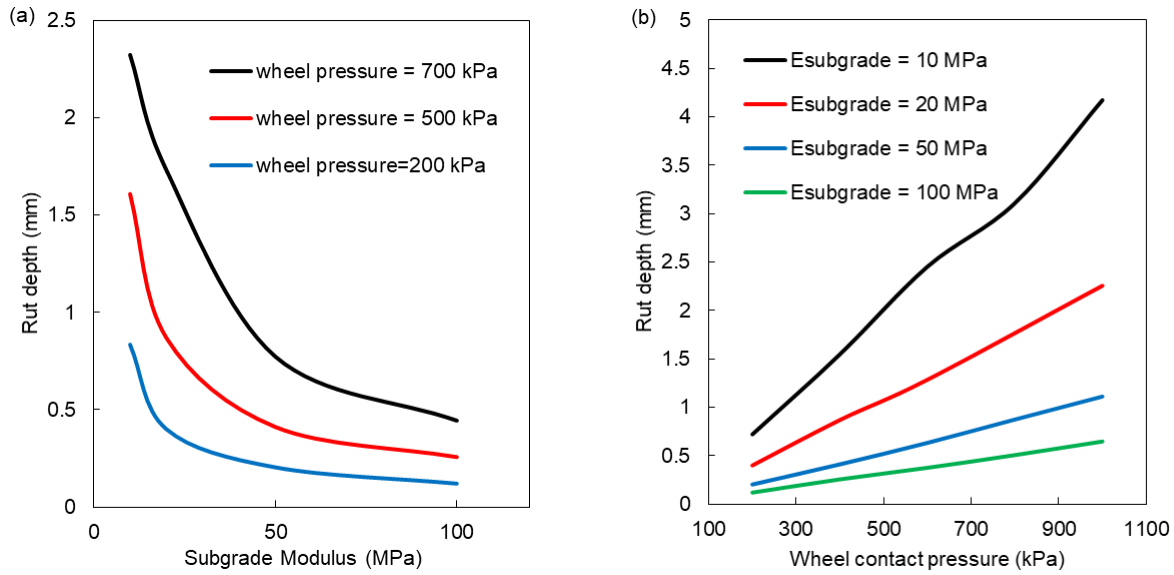

Figure 2. *Effect of wheel contact pressure on Rut depth (left), and effect of Subgrade Modulus on Rut depth (right)*

Figure 3a shows the rut depth estimation based on the CBR values, which were calculated using the empirical relation given by Klomp (1962) and Powell et al. (1984). Table-3 summarizes the range of rut depth studies by various researchers. Figure 3b shows the variation of rut depth along the geogrid stiffness (100-900 kN/m) for CBR values of 1 and 2%. The 1% CBR showed the uniform rut depth variation for the entire range (100-900 kN/m) of geogrid stiffness. The improved 2% CBR indicated a significant variation in the rut depth for lower geogrid stiffness. The geogrid thickness of 2 to 4 mm (Adams et al. 2014) was used to study the effect of geogrid stiffness for subgrade modulus of 10 and 20 MPa. A minute change is observed in the rut depth for the geogrid stiffness ranges from 100 to 900 kN/m.

Table 3. *Rut depth estimated from the various studies*

Past studies	Rut depth (mm)
Barksdale (1972)	12.7
Lister and Addis (1977)	12.7
AASHTO Joint Task (1989)	8.5-12.7
Sousa et al. (1991)	5.1
Hicks et al. (2000)	6-13
ASTM (2008)	1.6

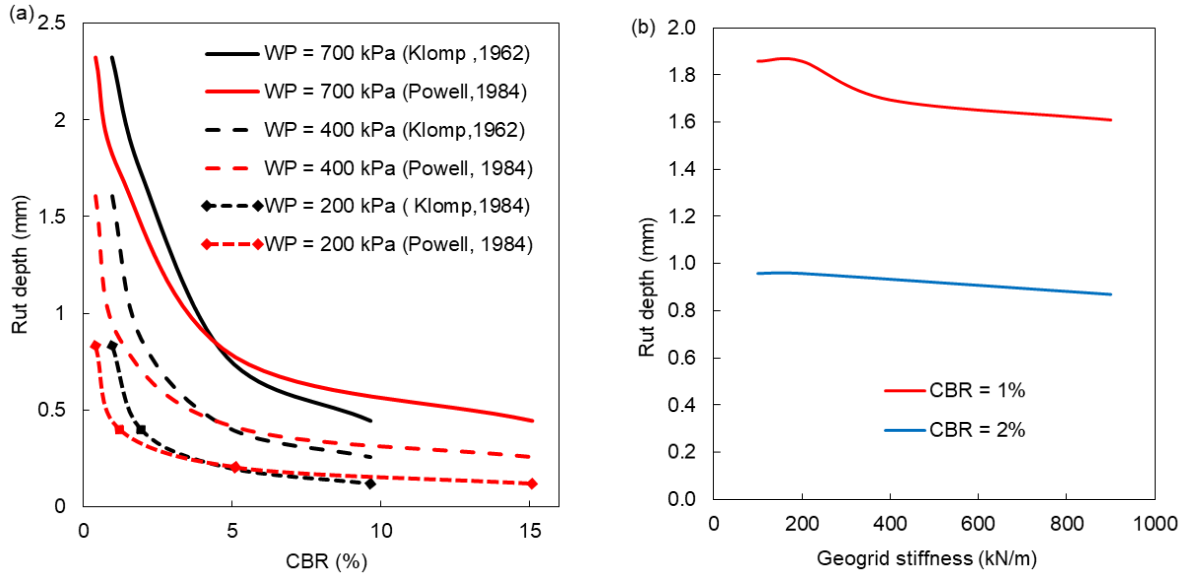

Figure 3. *Rut depth dependency on CBR (left), Effect of Geogrid stiffness on Rut depth under the wheel load of 400 kPa (right)*

4 CONCLUSIONS

The present study used finite element modeling to estimate the rut depth for the various subgrade modulus, contact pressure, and geogrid stiffness. The output results of ABAQUS software show the beneficial effect of the appropriate range of geogrid stiffness in the asphalt concrete layer. Parametric analysis was conducted to establish the optimal use of geogrid and subgrade stiffness values. Based on the result obtained in this study, the following points can be summarized.

(1) Vertical surface deformation is comparable with the experimental result (Correia et al. 2018) under the contact pressure of 350 kPa in axisymmetry finite element modeling.
(2) The effect of subgrade modulus on the rut depth for various contact pressure is analyzed. The significant dependency of rut depth on the subgrade modulus for 350 kPa contact pressure is observed.
(3) Maximum reduction in the rut depth is achieved for the subgrade modulus of 20 MPa for the entire geogrid stiffness of 100 kN/m to 900 kN/m.
(4) The presence of geogrid is observed in the displacement profile just below contact pressure in the sub-base layer of pavement.

5 ACKNOWLEDGEMENTS

The author appreciates the support provided by IIT Gandhinagar. Special thanks to Prof. Amit Prashant for his guidance and support.

REFERENCES

Adlinge, S. S., & Gupta, A. K. (2013). Pavement deterioration and its causes. *International Journal of Innovative Research and Development*, *2*(4), 437-450.

Abu-Farsakh, M. Y., Gu, J., Voyiadjis, G. Z., & Chen, Q. (2014). Mechanistic–empirical analysis of the results of finite element analysis on flexible pavement with geogrid base reinforcement. International Journal of Pavement Engineering, 15(9), 786-798

Adams, C. A., Amofa, N. Y., & Boahen, R. O. (2014). Effect of Geogrid Reinforced Subgrade on Layer Thickness Design of Low Volume Bituminous Sealed Road Pavements. IRJES, 3, 59-67

Al-Jumaili, M. (2016). Finite element modelling of asphalt concrete pavement reinforced with geogrid by using 3-D plaxis software. International Journal of Materials Chemistry and Physics, 2(2), 62-70

Arias, J. L., Inti, S., & Tandon, V. (2020). Influence of geocell reinforcement on bearing capacity of low-volume roads. *Transportation in Developing Economies*, *6*, 1-10.

Ari, A., & Misir, G. (2021). Three-dimensional numerical analysis of geocell reinforced shell foundations. *Geotextiles and Geomembranes*, *49*(4), 963-975.

Berg, R. R. (2000). Geosynthetic Reinforcement of the Aggregate Base/Subbase Courses of Pavement Structures

Behiry, A. E. A. E. M. (2012). Fatigue and rutting lives in flexible pavement. *Ain Shams Engineering Journal*, *3*(4), 367-374.

Collin, J. G., Kinney, T. C., & Fu, X. (1996). Full scale highway load test of flexible pavement systems with geogrid reinforced base courses. Geosynthetics International, 3(4), 537-549

Correia, N. S., Esquivel, E. R., & Zornberg, J. G. (2018). Finite-element evaluations of geogrid-reinforced asphalt overlays over flexible pavements. Journal of Transportation Engineering, Part B: Pavements, 144(2), 04018020.

Goud, G. N., Ramu, B., Umashankar, B., Sireesh, S., & Madhav, M. R. (2020). Evaluation of layer coefficient ratios for geogrid-reinforced bases of flexible pavements. Road Materials and Pavement Design, 1-12

Hegde, A., & Sitharam, T. G. (2015). 3-Dimensional numerical modelling of geocell reinforced sand beds. *Geotextiles and Geomembranes*, *43*(2), 171-181.

Kodippily, S., Yeaman, J., Henning, T., & Tighe, S. (2020). Effects of extreme climatic conditions on pavement response. *Road Materials and Pavement Design*, *21*(5), 1413-1425.

Maheshwari, P., & Babu, G. S. (2017). Nonlinear deformation analysis of geocell reinforcement in pavements. *International Journal of Geomechanics*, *17*(6), 04016144.

Perkins, S. W., Ismeik, M., & Fogelsong, M. L. (1999). Influence of geosynthetic placement position on the performance of reinforced flexible pavement systems (No. Volume 1)

Perkins, S. W., Christopher, B. R., Cuelho, E. L., Eiksund, G. R., Schwartz, C. S., & Svanø, G. (2009). A mechanistic–empirical model for base-reinforced flexible pavements. International Journal of Pavement Engineering, 10(2), 101-114

Pandey, S., Rao, K. R., & Tiwari, D. (2012, September). Effect of geogrid reinforcement on critical responses of bituminous pavements. In ARRB Conference, 25th, 2012, Perth, Western Australia, Australia

Sprague, C. J., Lothspeich, S., Chuck, F., & Goodrum, R. (2004). Geogrid Reinforcement of Road Base Aggregate—Measuring the Confinement Benefit. Geotechnical Engineering for Transportation Projects, 996-1005

Siriwardane, H., Gondle, R., & Kutuk, B. (2010). Analysis of flexible pavements reinforced with geogrids. Geotechnical and Geological Engineering, 28(3), 287-297

Suku, L., Prabhu, S. S., Ramesh, P., & Babu, G. S. (2016). Behavior of geocell-reinforced granular base under repeated loading. *Transportation Geotechnics*, *9*, 17-30.

Saride, S., & Baadiga, R. (2021). New Layer Coefficients for Geogrid-Reinforced Pavement Bases. Indian Geotechnical Journal, 51(1), 182-196

Sprague, C. J., Lothspeich, S., Chuck, F., & Goodrum, R. (2004). Geogrid Reinforcement of Road Base Aggregate—Measuring the Confinement Benefit. *Geotechnical Engineering for Transportation Projects*, 996-1005.

Transportation Officials. (1993). AASHTO Guide for Design of Pavement Structures, 1993 (Vol. 1). Aashto

Taherkhani, H., & Jalali, M. (2017). Investigating the performance of geosynthetic-reinforced asphaltic pavement under various axle loads using finite-element method. *Road Materials and Pavement Design*, *18*(5), 1200-1217.

Witczak, M. W. (2005). Simple performance tests: Summary of recommended methods and database (Vol. 46). Transportation Research Board